Effects of clustering and dimensionality on the magnetic properties of diluted magnetic semiconductors

R. N. Bhatt[1], Malcolm. P. Kennett[2], Mona Berciu[3] and Adel Kassaian[3]

[1] Department of Electrical Engineering, Princeton University, Princeton, NJ 08544, USA.
[2] Cavendish Laboratories, University of Cambridge, Madingley Rd, Cambridge CB3 0HE, UK.
[3] Department of Physics and Astronomy, University of British Columbia, Vancouver, BC V6T 1Z1, Canada.

ABSTRACT

The magnetic properties of films of diluted magnetic semiconductors (DMS) such as (Ga,Mn)As, as well as bulk grown crystals of similar materials, have been found to be extremely sensitive to growth conditions, both in terms of the ferromagnetic transition temperature, and the details of their magnetization curves. We study an impurity band model for carriers in Mn-doped DMS applicable in the low carrier density regime, and discuss the effects of clustering on the magnetic properties of DMS, using both numerical mean field and Monte Carlo simulations. In addition, we study the effects of dimensionality on the transition temperature and other magnetic behaviour, and compare our results with experimental data.

INTRODUCTION

The recent discovery of ferromagnetic diluted magnetic semiconductors (DMS) has led to intense research on their magnetic and transport properties motivated by their potential for use in spintronic devices [1]. $Ga_{1-x}Mn_xAs$ has been the most widely studied DMS [2], and has been found to have a Curie temperature (T_c) as high as 150 K [3,4] for bulk samples. An even higher $T_c = 172$ K [5] has been reported in a δ-doped heterostructure. It has been found that both the Curie temperature and also transport properties are very sensitive to the sample growth conditions. In particular, post-growth annealing has been used to consistently raise T_c by removing defects and was used to achieve the highest values of T_c mentioned above [3,6]. Other DMS with even higher T_c have been discovered (see. e.g. Refs. [7-10]), and applications such as gate-controlled ferromagnetism have been demonstrated [11], suggesting there are many more exciting developments in store.

The interesting magnetic properties of DMS have stimulated considerable theoretical interest in describing the physics of ferromagnetism and a large number of suggestions have been put forward [12-18]. The ferromagnetism in III-V DMS is widely accepted to be mediated by the antiferromagnetic exchange coupling between the charge carriers (holes) and the Mn spins [12]. Mn is an acceptor in GaAs when it substitutes for Ga, and hence one naively expects

the Mn and charge carrier concentrations to be equal. However, compensation processes such as As antisites and Mn interstitials [19-21] often lead to a hole concentration much less than that of Mn (of the order 10-30%). The main trends that all theories agree on are that for low x and carrier concentration, T_c monotonically increases with increasing x and hole concentration.

The low carrier and Mn concentrations in bulk DMS imply that there are likely to be relatively large spatial fluctuations in their magnetic properties due to the presence of spatial disorder in the Mn ion positions, i.e. clustering of Mn atoms. Initial approaches to the theory of DMS neglected the effects of disorder in mean field approximations [12,13,22], but more recently there has been considerable attention to these issues [14,23-29]. The changes in behavior that are found when disorder is included are that the shape of the magnetization versus temperature curve becomes highly unusual – concave upwards instead of convex, and T_c is enhanced relative to an ordered lattice of Mn [14,30].

In addition to the clustering induced through random positions of Mn ions, it is also possible to exert control over the Mn positions through the growth (using MBE) of layers of MnAs or (Ga,Mn)As in δ-doped heterostructures [31,32]. The aim of this work has been to increase the Mn concentration in the layers and then hopefully increase T_c due to the presence of large numbers of holes and Mn spins localized in the layer. The Mn concentration in the layer is generally much more than in the random alloy, e.g. 1/2 a monolayer (ML) of MnAs to 10 ML of GaAs, an overall fraction $x = 0.05$, but with a very different spatial distribution. Most experimental and theoretical work on layered structures has been for high Mn density, but there has also been some experimental work in which several ML of (Ga,Mn)As were grown with GaAs spacers, where $x = 0.04$ or 0.07 in the alloy regions [33]. A bilayer geometry with $x = 0.05$ in each layer was also studied theoretically by Boselli *et al.* [34]. In practice, even in the 1/2 ML systems, the Mn spins are found to reside over 3-5 ML [31,35], so that the fluctuation effects of the dilute limit may have some relevance to these high density layers as well.

The high Mn concentration case has been considered by several theorists [36-38], and the general consensus has been that T_c should be enhanced relative to the bulk alloy for the same overall Mn concentration. Experimentally, this appears to be the case, since the highest T_c reported thus far is in a δ doped sample [5]. Studies of the effect of spacer thickness in the high coverage limit have found that as the spacer thickness is decreased, T_c decreases monotonically until it is independent of spacer thickness, at which point, the layers appear to behave as independent magnetic layers [31]. In low Mn density samples, there was a suggestion of an oscillatory behaviour in T_c as a function of spacer thickness, which was speculated to be indicative of RKKY-like oscillations in the exchange [33]. As with the random alloy, there appears to be a strong correlation between magnetic and transport properties, with the more metallic transport corresponding to the highest T_c's [5], but as in the bulk case, these planar metals are quite dirty [38] with high residual resistivity at low temperatures. Very recent experiments also suggest that the sensitivity of magnetism to the local charge distribution as predicted in bulk (Ga,Mn)As [14,30], also appears

to occur in individual layers. Kreutz *et al.* [39] found that when they adsorbed a monolayer of organic molecules on the surface of a device with a single 0.5 ML of MnAs, the order in the pattern the organic molecules formed on the surface strongly influenced the Curie temperature – there was a large reduction in T_c for an ordered pattern and much less for a disordered pattern. More recent experiments have probed even lower dimensions – such as magnetoresistance in (Ga,Mn)As wires [40], and there have been theoretical studies of semiconductors with embedded DMS quantum dots [41].

We study the effects of spatial disorder in bulk samples and dimensionality in layered samples. The model we use incorporates the effects of spatial disorder for carriers that arise from an impurity band. In this approach the charge carriers are restricted to impurity (hydrogen-like) states trapped around each Mn acceptor [14,30]. The presence of an impurity band in $Ga_{1-x}Mn_xAs$ has been confirmed in ARPES measurements, in which the Fermi energy was found to lie in the impurity band [42-44] for $x \simeq 0.03$. Infra-red spectroscopy data is also consistent with an impurity band [45].

An impurity band model naturally explains the two orders of magnitude difference in the T_c of III-V based DMS ($\sim 10^2$ K) and II-VI based DMS ($\sim 10^0$ K) at low hole densities. One order of magnitude arises from the nature of the Bloch wave part of the valence band, which resides primarily on the anion (Group V/VI element), and more so in the case of II-VI than in III-V [46]. The other order of magnitude is due to the higher amplitude of an impurity-like state on the magnetic sites in the III-V case, where it is at the center of the envelope function, compared with the II-VI DMS, where the center of the envelope function is not at the isovalent Mn cation site, but at an independent dopant site (usually on the anion, though that is not crucial). Such an extra enhancement is not present in valence band Bloch states used in perturbative treatments of carrier states [12,13,22,24].

Our impurity band model has the simplifying feature that the carriers are treated as being electron-like, in that they have spin$-\frac{1}{2}$ rather than the spin$-\frac{3}{2}$ holes that are found in $Ga_{1-x}Mn_xAs$, and hence we are unable to study spin-orbit interactions. However, we have investigated these phenomenologically elsewhere and find that they do not change qualitative features of the magnetic properties [47]. The model is most appropriate for the low Mn and hole concentration regime near and below the metal-insulator transition (MIT) at $x \simeq 0.035$, where disorder effects are likely to be most pronounced [23].

We first introduce the impurity band model and then discuss our solutions of it using mean field (MF) theory and Monte Carlo simulations for both bulk samples and lower dimensional geometries. We find that disorder and low carrier concentrations lead to unusually shaped magnetization curves and an inhomogeneous ferromagnetic state. Spatial disorder in the Mn ion positions is also found to increase the Curie temperature relative to that found in ordered systems. We look at the effects of changing dimensionality, by comparing the magnetic properties of bulk, single layer and superlattice structures of (Ga,Mn)As. Our work here is most relevant to the experimental situation in Ref. [33]. Finally, we summarize our results and discuss their implications for the theoretical understanding of clustering and dimensionality effects in DMS.

IMPURITY BAND MODEL

We consider N_d spins $\mathbf{S}_i$ (Mn is spin-$\frac{5}{2}$, which we consider in the MF approximation (MFA), but we use classical spins in our Monte Carlo simulations for technical reasons), randomly placed on a fcc lattice (corresponding to the Ga fcc sublattice in GaAs) interacting with charge carriers which hop between the Mn sites, and described by the Hamiltonian

$$\mathcal{H} = \sum_{ij} t_{ij} c^\dagger_{i\sigma} c_{j\sigma} + \frac{1}{2} \sum_{ij} J_{ij} \mathbf{S}_i \cdot (c^\dagger_{j\alpha} \boldsymbol{\sigma}_{\alpha\beta} c_{j\beta}). \tag{1}$$

The hopping (t_{ij}) and exchange (J_{ij}) parameters are calculated with the assumption of $1s$ impurity states and depend on the separation between Mn ions exponentially, as described in Refs. [14,48]. (The length scale for the exponential decay is the Bohr radius $a_B = 7.8$ Å). We relate the Mn concentration $n_{\rm Mn}$ to the parameter $x = n_{\rm Mn} a^3/4$, where $a = 5.65$ Å is the GaAs lattice parameter, and we define p as the ratio of the hole and Mn concentrations.

MEAN FIELD ANALYSIS

We first solve the model specified in Eq. (1) using a mean field approximation for the exchange term,

$$\mathbf{S}_i \cdot \mathbf{s}_j \to \langle \mathbf{S}_i \rangle \cdot \mathbf{s}_j + \mathbf{S}_i \cdot \langle \mathbf{s}_j \rangle - \langle \mathbf{S}_i \rangle \cdot \langle \mathbf{s}_j \rangle \,,$$

where $\mathbf{s}_j = c^\dagger_{j\alpha} \boldsymbol{\sigma}_{\alpha\beta} c_{j\beta}$ is the carrier spin. Such a factorization requires the spins to lie in a single direction and hence suppresses thermal fluctuations.

We calculate the magnetization and the local charge carrier density for this model. The Mn magnetization is defined as

$$M(T) = \overline{\left\langle \frac{1}{N_d} \sqrt{\left| \sum_i \mathbf{S}_i \right|^2} \right\rangle}, \tag{2}$$

where $\langle \ldots \rangle$ is a thermal average and $\overline{\ldots}$ is an average over spatial disorder. The carrier magnetization is defined similarly. The results obtained for the magnetization as a function of temperature are shown in Fig. 1 for bulk samples.

Bulk samples

In Fig. 1, we demonstrate the effect of spatial disorder on the magnetization as a function of temperature, $M(T)$. For an ordered lattice of Mn spins, the $M(T)$ curve has a conventional, convex upward form.

In the totally random case, the $M(T)$ curve has a rather different shape, which is even convex upwards at low T, and has a much enhanced Curie temperature, T_c. We also consider intermediate levels of disorder that are labelled

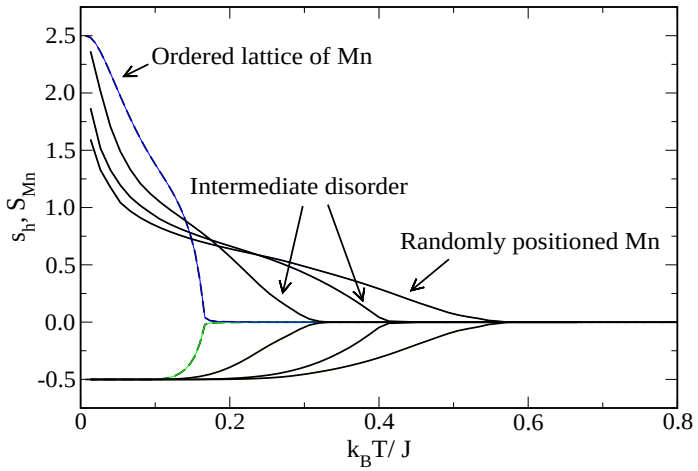

Figure 1: Mn magnetization (S_{Mn}) and carrier magnetization (s_h) as a function of temperature in the MFA for four different levels of disorder (labelled in the plot) for $x = 0.00926$ and $p = 0.1$. (Data from Ref. [14]).

in the figure, corresponding to allowing some disorder in the positions, but with constraints that keep the distribution from being completely random. Unsurprisingly, these show intermediate behavior, with less conventional $M(T)$ curves and higher T_c as disorder is increased.

Increasing either x or p leads to more conventional $M(T)$ curves and also leads to a higher Curie temperature. The effects of disorder are qualitatively similar to those found at lower x and p, even though T_c is not enhanced to the same degree as for low x and p. Two features left out of the impurity band model that one might expect to be present in a more realistic model, are on-site disorder, as might arise due to chemical disorder, and carrier-carrier interactions. These can be included, and for reasonable parameter values, neither affects the qualitative results outlined above significantly [48].

Layered samples

In Fig. 2 we present a summary of our MF data on layered structures. In panel a), we compare the $M(T)$ curves of a bulk sample with $x = 0.02$, $p = 0.1$ to that of individual layers with thickness $t = 2$, 4, and 5 unit cells and the same Mn and hole concentrations in each layer. As the thickness of the layer increases, the magnetism becomes more robust, and T_c increases. In panel b) we consider heterostructures with several different spacer distances, d, and compare them to a bulk sample.

As the spacer thickness is decreased, the $M(T)$ curve becomes more robust, but interestingly T_c appears not to be greatly affected. For $d \geq 5$ unit cells, the $M(T)$ curve changes little with increasing d, suggesting that in the MFA, the weakly-interacting layer limit is reached very quickly. We also found that if we

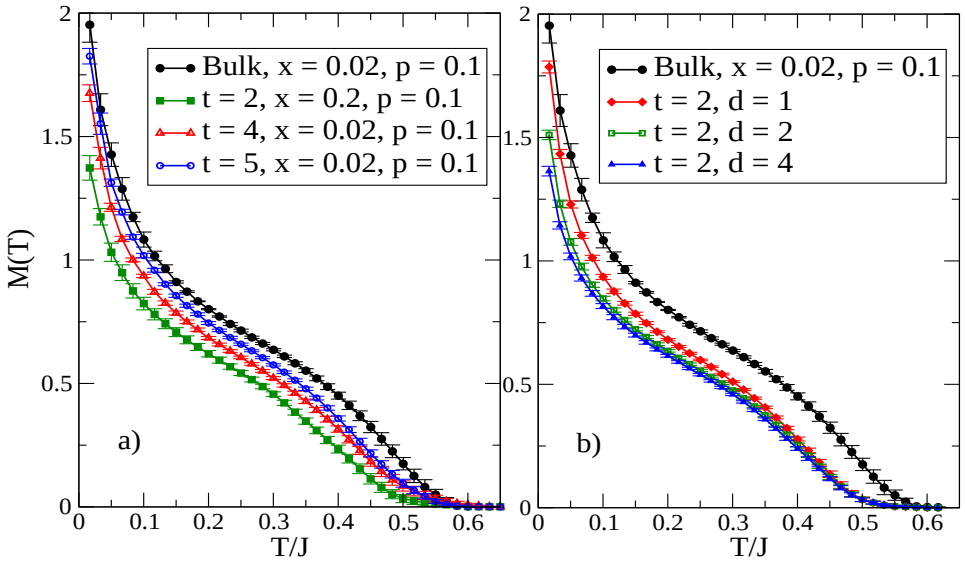

Figure 2: Mn magnetization as a function of temperature for a bulk sample with $x = 0.02$ and $p = 0.1$, compared with a) varying single layer thickness, $t = 2$, 4, and 5 unit cells, and b) a heterostructure with constant layer thickness $t = 2$ and varying spacing $d = 1$, 2, and 4 unit cells.

kept the number of spins fixed, then T_c increased as the layer thickness t was decreased. Note that the samples shown were not completely disordered – this was to reduce the amount of disorder averaging required in the simulations, and has the effect of reducing T_c, but should not qualitatively affect our investigation of dimensionality effects.

In 2 dimensions there is no expectation of long-range magnetic order due to the Mermin-Wagner theorem [49], but we do not consider a truly 2 dimensional system here and MF theory can impose order that is destroyed when fluctuations are taken into account.

MONTE CARLO CALCULATIONS

It is well known that the MFA overestimates T_c by neglecting thermal fluctuations which are of great importance in low dimensions. These fluctuations are included in a Monte Carlo simulation. In previous work we found that many of the findings of MF calculations are robust for the random alloy [30]. In particular, we found that unusual magnetization curves persist and agree qualitatively with experiments on insulating samples [50], and that T_c is higher in disordered samples than ordered samples with the same parameters.

In the MFA we were able to consider spin-$\frac{5}{2}$ Mn spins, but here we use classical spins so as to avoid quantum Monte Carlo simulations. These would be even more computationally intensive than the current calculations, and also unwarranted given the large value of S, implying small corrections of order $1/S$ as compared to quantum Monte Carlo results, and the level of accuracy to which input parameters of the model are known.

We calculated the Mn magnetization for bulk and layered samples and also the susceptibility for layered samples. We show $M(T)$ data for $x = 0.01$, 0.03 with $p = 0.1$, 0.3 in Fig. 3 for the bulk Mn magnetization. We find that increasing x and p lead to changes from concave upwards to linear $M(T)$ curves. Note that the magnetization curves do not go to zero at high temperatures, but to $1/\sqrt{N}$, where N is the number of spins – this is an effect of the relatively small number of spins used in the simulation – in the thermodynamic limit, these curves would go to zero at high temperatures.

We studied several layered systems; firstly a system with a thickness of $t = 10$ unit cells, and 80 Mn spins and 8 holes ($x = 0.02, p = 0.1$) – this lacked periodic boundary conditions in the z-direction – a "quasi-2d" layer. We also considered δ-doped heterostructures with $t = 5$ and $d = 3$, 5 and 10 unit cells. The $M(T)$ curves of these samples are shown and compared to the equivalent bulk case in Fig. 4 a). The equivalent bulk case for the "quasi-2d" layer is $x = 0.02$, $p = 0.1$, whilst for the $t = 5$, $d = 5$ system, the overall doping is $x = 0.01$, $p = 0.1$, even though it is $x = 0.02$ in the layer – we show this for comparison. As in the MF case, the $M(T)$ curves appear to be independent of d for $d \geq 5$.

Even though there is no true long range order in 2 dimensions, and hence no finite $M(T)$ at $H = 0$ for $T > 0$ for the 2 dimensional case in the *thermodynamic limit*, a small symmetry breaking field (H) or a 3 dimensional coupling (as we

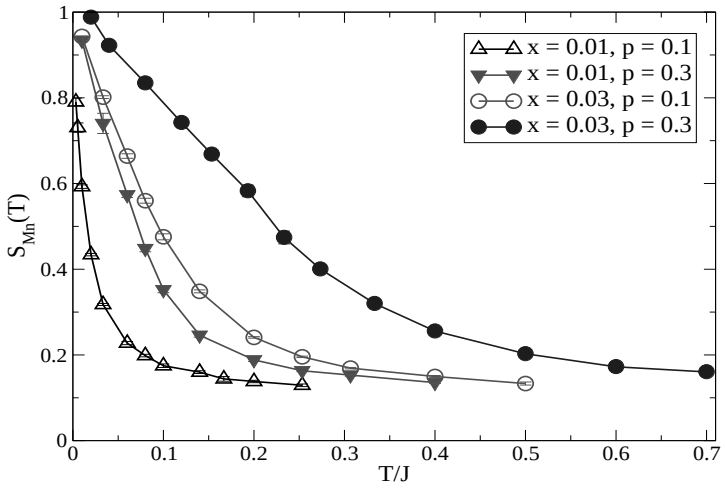

Figure 3: Mn magnetization (normalized to its saturation value) as a function of temperature for $x = 0.01$ and $x = 0.03$. The samples are insulating or near the MIT. (Data from Ref. [30]).

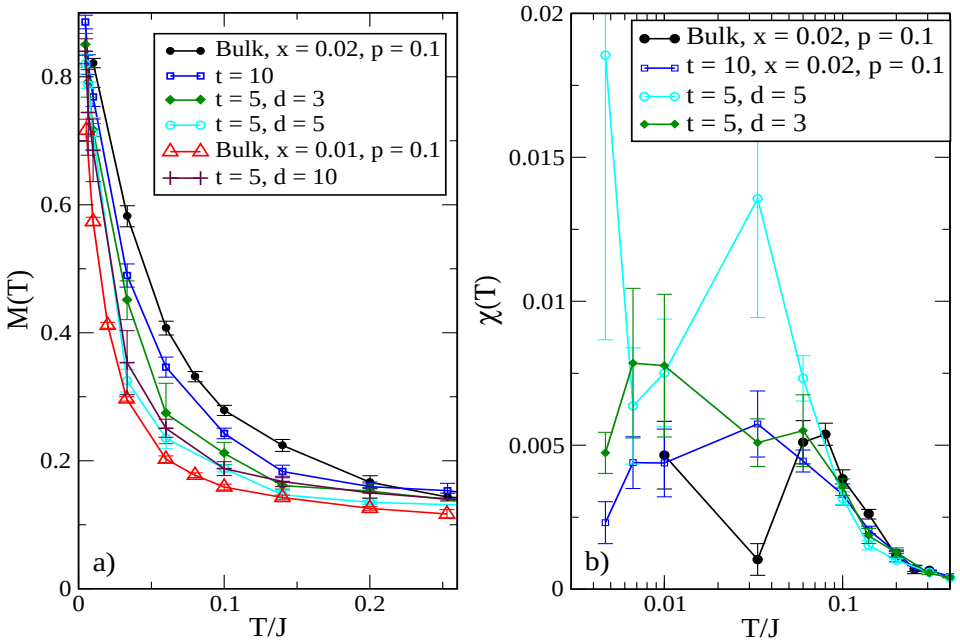

Figure 4: a) $M(T)$ and b) magnetic susceptibility curves for bulk samples with $p = 0.1$ and $x = 0.02$ and $x = 0.01$, compared with samples with a single layer of $t = 10$ and also $t = 5$, with $d = 3$, 5, and 10 , and $x = 0.02$, $p = 0.1$ within the layers.

have in our simulations of layered systems here) will produce a finite $M(T)$, as do the finite size effects associated with Monte Carlo simulations.

We also calculated the magnetic susceptibility for Mn and find significant weight both around T_c and at lower temperatures (see Fig. 4 b)) – we do not see a divergence at T_c due to the small size of our systems. We expect that the low temperature contribution is from "effectively free" spins, as has already been noted in Monte Carlo studies of bulk II-VI [51] and III-V DMS [30].

Our results can be summarized as follows – as in the MFA, the magnetization is smaller for a layered structure than the equivalent bulk one, however, a heterostructure enhances the magnetization relative to a random alloy with the same overall Mn concentration.

Spatially heterogeneous magnetism

In the bulk case we considered local quantities as well as global quantities such as the magnetization, in particular, the local carrier charge density on Mn sites, ρ_i and the local magnetization – the projection of each spin onto the global magnetization, M_i^{local}. We found that large local magnetizations and large local carrier densities are strongly spatially correlated as shown in Fig. 5.

This correlation between charge and magnetism arises from regions of higher Mn and carrier density coinciding, since the carriers can lower their energy

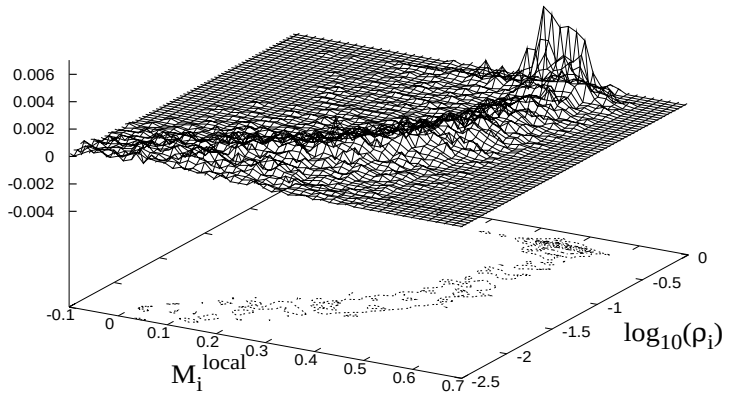

Figure 5: Joint probability distribution for local magnetization and charge density for $x = 0.01$, $p = 0.1$ calculated with $N_d = 110$ at $T = T_c/4$. Large local magnetizations correlate with large local charge carrier densities. (Ref. [30]).

through exchange interactions and hence "puddles" of ferromagnetism grow with decreasing temperature.

An inhomogeneous magnetic state as described above can lead to a higher T_c than found for an ordered lattice of Mn spins [14,23,30] as shown earlier. This occurs through regions of higher than average Mn density polarizing at temperatures above the T_c for an ordered system [30,52]. If there is enough communication between such regions, long-range order develops at a higher T_c than in the ordered case. We can thus separate the Mn spins into two classes – either seeing a large or a small charge density. This suggests a natural way to view the magnetism is in terms of strongly and weakly coupled populations of Mn spins [53]. It also suggests that the magnetic ordering takes place as a percolation transition. In reality, a distribution of couplings exists, but a two species model can be used to fit experimental data [53] even in the metallic phase, where one no longer expects two peaks in the distribution. It turns out that it is not so much the peaked structure of the distribution (which disappears with higher x and p), but its width (which disappears much more slowly) that leads to a two species model being useful.

Since we find an inhomogeneous magnetic state in the bulk, it is reasonable to expect that in small samples, such as nanostructures, such effects may be more pronounced. A similar mechanism might also be expected to apply to raise the T_c in a layered system, except that the "puddles" are defined in the growth intentionally. The two species approach described above may also be useful to fit the temperature and magnetic field depdendence of the magnetization in experiments involving digitally doped systems. The presence of many weakly coupled spins in dilute systems is similar to the bulk case, while in the high density case, one expects the strongly coupled spins to reside in the layers, and the weakly coupled spins to lie in the scatter around the monolayer [32].

CONCLUSIONS

Disorder can have important qualitative effects on ferromagnetism in DMS with low carrier concentrations. In an impurity band model for $Ga_{1-x}Mn_xAs$, we find that the ferromagnetic state is spatially inhomogeneous, due to spatial disorder in the positions of Mn spins and the low carrier concentration. This leads to unusually shaped magnetization curves and an enhanced Curie temperature relative to an ordered lattice of Mn spins. These results are confirmed in both mean field and Monte Carlo simulations. We also find that regions with large local magnetization are strongly correlated with regions of large carrier density. We find that the shape of the magnetization curve is sensitive to disorder as well as carrier concentration. Further study of the shape of these curves over the entire temperature range, not just to determine T_c, will lead to further insights into ferromagnetism in DMS, as advocated recently by Das Sarma *et al.* [54]. Such variation in the shape of the $M(T)$ curves leaves open the possibility of engineering the shape of such curves for specific applications.

We find many similarities between the magnetic properties of bulk and layered samples. As in experiments on heterostructures, we find that increasing the spacing between layers decreases the robustness of magnetism, but that at large spacer size, d, the magnetic properties become independent of d. We also find that the magnetization is stronger than in a bulk sample with equivalent overall Mn doping. The presence of significant weight in the susceptibility at low temperature is indicative of many weakly coupled spins, that arise from a combination of disorder and low dimensionality.

Despite the rapid progress in this field in recent years, there are still many unresolved questions as to the nature of the ferromagnetic state, in particular the roles of various defects and different experimental geometries. Advancements in experimental techniques and new materials will hopefully allow a clearer picture to emerge in the next few years.

ACKNOWLEDGEMENTS

We acknowledge useful discussions with Stefano Sanvito, Chenggang Zhou and Xin Wan. This work was supported by NSF DMR-9809483, NSF DMR-0213706, and the NSERC.

REFERENCES

1. G. Prinz, Science **282**, 1660 (1998); H. Ohno, Science **281**, 951 (1998); S. J. Pearton, C. R. Abernathy, D. P. Norton, A. F. Hebard, Y. D. Park, L. A. Boatner, and J. D. Budai, Mat. Sci. Eng. R **40**, 137 (2003).
2. H. Ohno and F. Matsukura, Solid State Commun. **117**, 179 (2001).

3. K. W. Edmonds, K. Y. Yang, R. P. Campion, A. C. Neumann, N. R. S. Farley, B. L. Gallagher, and C. T. Foxon, Appl. Phys. Lett. **81**, 4991 (2002).
4. K. C. Ku, S. J. Potashnik, R. F. Wang, S. H. Chun, P. Schiffer, N. Samarth, M. J. Seong, A. Mascarenhas, E. Johnston-Halperin, R. C. Myers, A. C. Gossard, and D. D. Awschalom, Appl. Phys. Lett. **82**, 2302 (2003).
5. A. M. Nazmul, S. Sugahara, and M. Tanaka, Phys. Rev. B **67** 241308(R) (2003).
6. S. J. Potashnik, K. C. Ku, S. H. Chun, J. J. Berry, N. Samarth, and P. Schiffer, Appl. Phys. Lett. **79**, 1495 (2001).
7. N. Theodoropoulou, A. F. Hebard, S. N. G. Chu, M. E. Overberg, C. R. Abernathy, S. J. Pearton, R. G. Wilson, and J. M. Zavada, Appl. Phys. Lett. **79**, 3542 (2001).
8. S. G. Cho, S. Choi, S. C. Hong, Y. Kim, J. B. Ketterson, B. J. Kim, Y. C. Kim, and J. H. Jung, Phys. Rev. B **66**, 033303 (2002).
9. Y. D. Park, A. T. Hanbicki, S. C. Erwin, C. S. Hellberg, J. M. Sullivan, J. E. Mattson, T. F. Ambrose, A. Wilson, G. Spanos, and B. T. Jonker, Science **295**, 651 (2002).
10. K. Sato, G. A. Medvedkin, T. Nishi, Y. Hasegawa, R. Misawa, K. Hirose, and T. Ishibashi, J. Appl. Phys. **89**, 7027 (2001).
11. H. Ohno, D. Chiba, F. Matsukura, T. Omiya, E. Abe, T. Dietl, Y. Ohno, and K. Ohtani, Nature **408**, 944 (2000).
12. T. Dietl, H. Ohno, F. Matsukura, J. Cibert, and D. Ferrand, Science **287**, 1019 (2000).
13. J. König, H.-H. Lin, and A. H. MacDonald, Phys. Rev. Lett. **84**, 5628 (2000).
14. M. Berciu and R. N. Bhatt, Phys. Rev. Lett. **87**, 107203 (2001).
15. A. Chattopadhyay, S. Das Sarma, and A. J. Millis, Phys. Rev. Lett. **87**, 227202 (2001).
16. S. Sanvito, N. A. Hill and P. Ordejón, Phys. Rev. B **63**, 165206 (2001).
17. A. Kaminski and S. Das Sarma, Phys. Rev. Lett.**88**, 247202 (2002).
18. G. Zarand and B. Janko, Phys. Rev. Lett. **89**, 047201 (2002).
19. S. Sanvito and N. A. Hill, Appl. Phys. Lett. **78**, 3493 (2001).
20. K. M. Yu, W. Walukiewicz, T. Wojtowicz, I. Kuryliszyn, X. Liu, Y. Sasaki, and J. K. Furdyna, Phys. Rev. B **65**, 201303 (2002).
21. S. C. Erwin and A. G. Petukhov, Phys. Rev. Lett. **89**, 227201 (2002).
22. T. Dietl, H. Ohno, and F. Matsukura, Phys. Rev. B **63**. 195205 (2001).
23. R. N. Bhatt, M. Berciu, M. P. Kennett, and X. Wan, J. Supercond. **71**, 15 (2002).
24. J. Schliemann, J. König, and A. H. MacDonald, Phys. Rev. B **64**, 165201 (2001).
25. A. L. Chudnovskiy and D. Pfannkuche, Phys. Rev. B **65**, 165216 (2002).
26. S. R. E. Yang and A. H. MacDonald, Phys. Rev. B **67**, 155202 (2003).
27. G. Bouzerar, J. Kudrnovsky, L. Bergqvist, and P. Bruno, Phys. Rev. B **68**, 081203 (2003).
28. D. J. Priour, E. H. Hwang, and S. Das Sarma, cond-mat/0305413.
29. C. Timm, cond-mat/0311029.

30. M. P. Kennett, M. Berciu, and R. N. Bhatt, Phys. Rev. B **66**, 045207 (2002).
31. R. K. Kawikami, E. Johnston-Halperin, L. F. Chen, M. Hanson, N. Guebels, J. S. Speck, A. C. Gossard, and D. D. Awschalom, Appl. Phys. Lett. **77**, 2379 (2000).
32. E. Halperin-Johnston, J. A. Schuller, C. S. Gallinat, T. C. Kreutz, R. C. Myers, R. K. Kawakami, H. Knotz, A. C. Gossard, and D. D. Awschalom, Phys. Rev. B **68**, 165328 (2003).
33. R. Mathieu, P. Svedlindh, J. Sadowski, K. Świątek, M. Karlsteen, J. Kanski, and L. Ilver, Appl. Phys. Lett. **81**, 3013 (2002).
34. M. A. Boselli, I. C. da Cunha Lima, and A. Ghazali, Phys, Rev. B **68**, 085319 (2003).
35. T. C. Kreutz, G. Zanelatto, E. G. Gwinn, and A. C. Gossard, Appl. Phys. Lett. **81**, 4766 (2002).
36. J. Fernández-Rossier and L. J. Sham, Phys. Rev. B **66**, 073312 (2002); Phys. Rev. B **64**, 235323 (2001).
37. I. Vurgaftman, and J. R. Meyer, Phys. Rev. B **64**, 245207 (2001).
38. S. Sanvito, Phys. Rev. B **68**, 054425 (2003).
39. T. C. Kreutz, E. G. Gwinn, R. Artzi, R. Naaman, H. Pizem, and C. N. Sukenik, Appl. Phys. Lett. **83**, 4211 (2003).
40. C. Rüster, T. Borzenko, C. Gould, G. Schmidt, L. W. Molenkamp, X. Liu, T. J. Wojtowicz, J. K. Furdyna, Z. G. Yu, and M. E. Flatté, Phys. Rev. Lett. **91**, 216602 (2003).
41. P. Lyu and K. Moon, cond-mat/0210643.
42. J. Okabayashi, A. Kimura, O. Rader, T. Mizokawa, A. Fujimori, T. Hayashi, and M. Tanaka, Physica E (Amsterdam) **10**, 192 (2001).
43. J. Okabayashi, A. Kimura, O. Rader, T. Mizokawa, A. Fujimori, T. Hayashi, and M. Tanaka Phys. Rev. B **64**, 125304 (2001).
44. H. Asklund, L. Ilver, J. Kanski, J. Sadowski, and R. Mathieu, Phys. Rev. B **66**, 115319 (2002).
45. E. J. Singley, K. S. Burch, R. Kawikami, J. Stephens, D. D. Awschalom, and D. N. Basov, Phys. Rev. B **68**, 165204 (2003).
46. D. J. Chadi, Phys. Rev. B **16**, 3572 (1977); *ibid* **19**, 2074 (1979).
47. C. Zhou, M. P. Kennett, X. Wan, M. Berciu, and R. N. Bhatt, cond-mat/0310322.
48. M. Berciu and R. N. Bhatt, cond-mat/0111045.
49. N. D. Mermin and H. Wagner, Phys. Rev. Lett. **17**, 1133 (1966).
50. B. Beschoten, P. A. Crowell, I. Malajovich, D. D. Awschalom, F. Matsukura, and H. Ohno, Phys. Rev. Lett. **83**, 3073 (1999).
51. R. N. Bhatt and X. Wan, Int. J. Mod. Phys. C **10**, 1459 (1999); X. Wan and R. N. Bhatt, cond-mat/0009161.
52. M. Mayr, G. Alvarez, and E. Dagotto, Phys. Rev. B **65**, 241202(R) (2002).
53. M. P. Kennett, M. Berciu, and R. N. Bhatt, Phys. Rev. B **65**, 115308 (2002).
54. S. Das Sarma, E. H. Hwang, and A. Kaminski, Phys Rev. B **67**, 155201 (2003).